Desalination and Water Treatment
www.deswater.com

1 (2009) 312–317

1944-3994 / 1944-3986

Laboratory studies and CFD modeling of photocatalytic degradation of colored textile wastewater by titania nanoparticles

Niyaz Mohammad Mahmoodi[a*], Mokhtar Arami[b], Kamaladin Gharanjig[a]

[a]*Department of Environmental Research, Institute for Colorants, Paint and Coatings, Tehran, Iran*
Tel. +98 021 22956126; Fax +98 021 22947537; email: mahmoodi@icrc.ac.ir
[b]*Textile Engineering Department, Amirkabir University of Technology, Tehran, Iran*

Received 15 February 2008; accepted revised 19 July 2008

ABSTRACT

This paper presents photocatalytic decolorization, computational fluid dynamics (CFD) modeling of decolorization and mineralization of textile dyes, Astrason Blue FGGL (AB) and Solophenyl Yellow FFL (SF), by photocatalysis using immobilized titania nanoparticle. UV-Vis spectrophotometry, Ion chromatography (IC) and total organic carbon (TOC) analyses were employed to obtain the details of the photocatalytic decolorization and mineralization of AB and SF. The CFD model was used to solve the mathematical equation describing decolorization process numerically taking into account finite volume descretization scheme. The CFD model predictions were compared to those results obtained from experimental tests for the decolorization of dyes by photocatalysis and close agreement was achieved. Ninety-five percent total organic carbon of both dyes can be eliminated after 240 min of irradiation time.

Keywords: Photocatalysis; CFD modeling; Decolorization; Mineralization; Titania nanoparticle

1. Introduction

The problems associated with the discharge of wastewater from various industries such as textile, paper, food, plastics and cosmetics have concerned both industrial and academic scientists. These wastewaters cause many significant problems such as increasing the toxicity of the effluent, skin irritation and cancer to humans, also reducing the light penetration that has a derogatory effect on photosynthesis phenomenon. From the aesthetical point of view, the presence of organics in particular, carcinogenic compounds in the receiving surface and under ground waters are not safe, pleasant and welcome [1–10].

Photocatalysis constitutes one of the emerging technologies for the degradation of organic pollutants [11–24]. Several advantages of this process over competing processes are: complete mineralization, no waste-solids disposal problem, and only mild temperature and pressure conditions are necessary [11–14]. Titania is a material with excellent merits in UV energy transferring and photocatalysis of poison compounds in environment. Further, the strong oxidizing power of the photogenerated holes, the chemical inertness, and the non-toxicity of TiO_2 has also made it a superior photocatalyst [25–29].

Although many experimental works have been conducted to assess the capability and the performance of photocatalysis for the degradation of dyes from the textile industry, little research has been done to model dye-removal process from the textile wastewaters and to evaluate the significance of the effect of major parameters on the percent of dye adsorption. There are more recent papers involving model on the other area [30–32].

The aim of the present study is to investigate the photocatalytic decolorization, computational fluid dynam-

* Corresponding author.

ics modeling of decolorization and minerlization of Astrason Blue FGGL (AB) and Solophenyl Yellow FFL (SF) using an immobilized TiO_2 particle photocatalytic reactor. The CFD model was used to solve the mathematical equation describing decolorization process numerically taking into account finite volume descretization scheme.

2. Experimental

Astrason Blue FGGL (AB) and Solophenyl Yellow FFL (SF) were obtained from Bayer AG and Ciba respectively. The descriptions of AB and SF are shown in Table 1.

Titania (Degussa P25) was utilized as a photocatalyst. Its main physical data are as follows: average primary particle size around 30 nm, purity above 97% and with 80:20 anatase to rutile. Other chemicals were purchased from Merck.

Experiments were carried out in an immersion rectangular immobilized TiO_2 particle photocatalytic reactor made of Pyrex glass. A simple and effective method was used for the immobilization of TiO_2 particles as follows: Inner surfaces of reactor walls were cleaned with acetone and distilled water to remove any organic or inorganic material attached to or adsorbed on the surface and was dried in the air. A pre-measured mass of TiO_2 (16 g) was attached on the inner surfaces of reactor walls using a thin layer of a UV resistant polymer. Immediately after preparation, the inner surface reactor wall–polymer–TiO_2 particle system was placed in the laboratory for at least 60 h for complete drying of the polymer [33–35]. Two UV-C lamps (15 W, Philips) were used as the radiation source. An air pump was utilized for the mixing and aeration of dye solution.

Photocatalytic decolorization and mineralization processes were performed using a 7 L solution containing specified concentration of dye. Solutions were prepared using distilled water to minimize interferences. The initial concentration of AB and SF were 0.11 and 0.073 mM respectively. The photocatalytic degradation processes were carried out at 298 K. Samples were withdrawn from sample point at certain time intervals and analyzed for decolorization and mineralization.

AB and SF are azo dyes, which have strong absorbances in the UV-visible region. The chromophore part containing azo linkage (–N=N–) has an absorption in the visible region while benzene and heterocyclic rings in the UV region. Decolorization of dye solutions were checked and controlled by measuring the maximum absorbance at λ_{max} (600 and 387.5 nm for AB and SF respectively) of dye solutions at different time intervals by UV-Vis CECIL 2021 spectrophotometer.

Computational fluid dynamics modeling incorporating the finite volume descretization scheme is used to simulate the photocatalytic decolorization of the selected dyes.

Ion chromatograph (METROHM 761 Compact IC) was used to assay the appearance and quantity of formate, acetate, oxalate, SO_4^{2-} and NO_3^- ions formed during the decolorization and mineralization of the selected dyes using a METROSEP anion dual 2, flow 0.8 mL/min, 2 mM $NaHCO_3$/1.3 mM Na_2CO_3 as eluent, temperature 20°C, pressure 3.4 MPa and conductivity detector.

The total organic carbon (TOC) of the reaction solution was measured by a digester and Spectrophotometer DR/2500 (Hach).

Table 1
Properties of AB and SF

Parameter	AB	SF
Empirical formula	$C_{20}H_{26}N_4O_6S_2$	$C_{28}H_{18}N_4O_6S_4Na_2$
Formula weight (g/mol)	482	680
Company	Bayer AG	Ciba

3. Results and discussion

3.1. Decolorization and computational fluid dynamics modeling

Figs. 1a and 1b (dots) show the dye concentration as a function of the irradiation time when different H_2O_2 concentrations were used. It is shown to be exponential to irradiation time at each concentration of H_2O_2. This means that the first order kinetics relative to AB and SF is operative. The correlation coefficient (R^2) and degradation rate constants (k, 1/min) for the various H_2O_2 concentrations are shown in Table 2. Generally, the degradation rate of dye increases as the H_2O_2 concentration increases until an optimal concentration is achieved. However, at high concentration, H_2O_2 can also become a scavenger of valence bond holes and hydroxyl radicals [36].

Table 2
Parameters (k and R^2) for the effect of different H_2O_2 concentrations on the decolorization rate of AB and SF

H_2O_2 (mM)	AB		SF	
	k (1/min)	R^2	k (1/min)	R^2
0.5	—	—	0.002	0.982
1.5	0.012	0.994	—	—
2.5	—	—	0.012	0.987
4.5	0.041	0.994	—	—
5.0	—	—	0.050	0.988
7.3	0.052	0.993	—	—
7.5	—	—	0.054	0.993
9	—	—	0.058	0.980
10.5	0.057	0.998	—	—
13.5	0.058	0.995	—	—

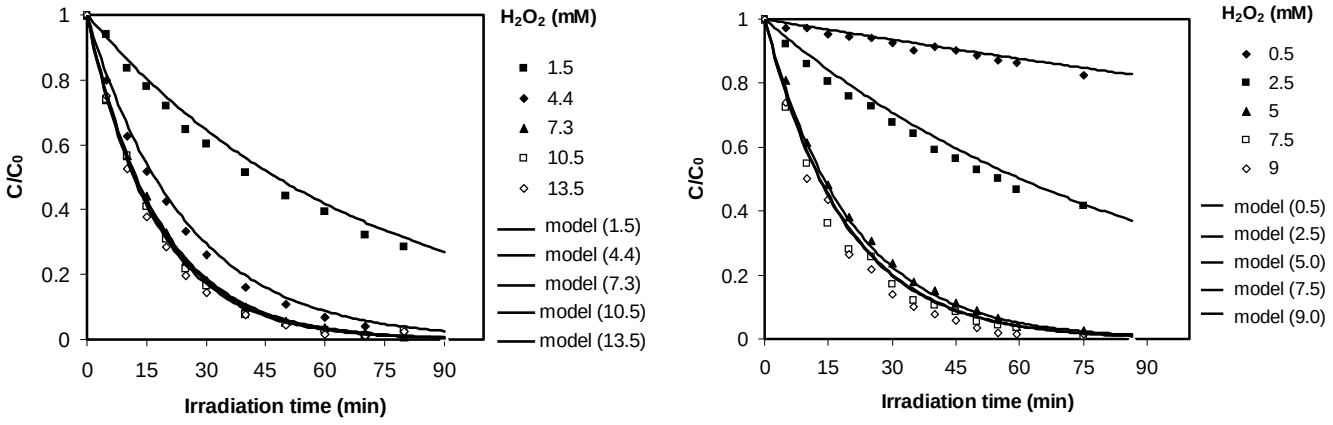

Fig. 1. Photocatalytic decolorization of (a) AB (b) SF (dots: experimental data, solid lines: model predictions for the relative concentrations of hydrogen peroxide) at different time intervals of irradiation (C_0 initial dye concentration and C dye concentration at time t).

In this paper a computational fluid dynamics model incorporating the finite volume descretization scheme is presented to simulate the photocatalytic decolorization of selected dyes using photocatalysis process. The partial differential equation describing the photocatalytic decolorization process is given in Eq. (1). This equation was numerically solved using PHOENICS package and incorporating finite volume integration scheme in order to simulate the decolorization from aqueous solution.

$$\partial C_1 / \partial t = D\partial^2 C_1 / \partial x^2 - kC_1 \quad (1)$$

where C_1 = dye concentration in aqueous system (mM), k = first-order rate constant (1/min), t = time (min), x = Cartesian coordinates (m) and D = diffusion coefficient (m^2/min).

The equation describing photocatalytic decolorization of dyes in solution phase was solved using the PHOENICS CFD package. PHOENICS is a general-purpose CFD package that can be used for simulation of fluid flow, heat transfer, and mass transfer processes. In the case of a single-phase problem, the partial differential equation solved by PHOENICS has the following general form [37]:

$$\partial(\rho\psi)/\partial t + \partial\left(\rho u_j \psi - \Gamma_\psi \partial\psi / \partial x_j\right)/\partial x_j = S_\psi \quad (2)$$

where ψ = any of the dependent variable, t = time, ρ = PHOENICS-term for density, u_j = velocity component in the x_j direction, Γ_ψ = diffusive exchange coefficient for ψ and S_ψ = source rate of ψ.

The general source term S_ψ can include all terms other than diffusion, convection and transient terms in the equation.

Since the model equation may contain terms which are not included in the PHOENICS general equation, they are implemented in PHOENICS by introducing the appropriate setting for each term in the Q1 file and applying extra FORTRAN coding in the GROUND subroutine.

In order to model the photocatalytic degradation of dyes from the solution phase, a one-dimensional simulation was performed using PHOENICS package. The model input data are given in Table 3.

A one-dimensional finite volume model with a reactor length of 380 mm was divided into 50 equal size control volumes. The x-direction of Cartesian coordinate was used to simulate horizontal batch system in which photocatalytic decolorization process takes place. The number of time steps used was 12. Total iteration of 1000 was assigned to the simulation. The model was then run for a simulation time of 60 minutes. A molecular diffusion coefficient of 1×10^{-9} m^2/s was assigned for selected dyes dissolved in solution system. All model input data were set through the Q1 file of PHOENICS package.

Figs. 1a and 1b compare experimental data (dots) and model predictions (solid lines) of decolorization rates of

Table 3
Model input data used for the simulation of photocatalytic decolorization of dyes

Input parameter	Value
Initial dye concentration (mM)	AB: 0.11, SF: 0.073
Kinetic constant (1/min)	Table 2
Molecular diffusion (m^2/min)	1×10^{-9}
Number of iterations	1000
Number of time steps	12
PHOENICS-term for density (g/cm^3)	1.0
Differencing scheme	Hybrid

AB and SF, as a function of irradiation time at different hydrogen peroxide concentrations. The simulation results were then compared to those results obtained from experimental tests for the higher concentrations of H_2O_2 and close agreement was achieved. This can be explained by the scavenging effect of hydrogen peroxide when using a higher H_2O_2 concentration on the further generation of hydroxyl radicals in aqueous solution (7.3 and 5.0 mM for AB and SF respectively).

3.2. Mineralization of dyes

During the photocatalytic decolorization and mineralization of dye, various organic intermediates were produced. Consequently, destruction of the dye should be evaluated as an overall degradation process, involving the degradation of both the parent dye and its intermediates.

Further hydroxylation of aromatic intermediates leads to the cleavage of the aromatic ring resulting in the formation of oxygen-containing aliphatic compounds [38]. Formate, acetate and oxalate were detected as important aliphatic carboxylic acid intermediates during the degradation of AB and SF (Figs. 2a and 2b respectively). The formation of oxalate initially increased with the irradiation time, and then sharply dropped. After 240 min of irradiation, carboxylic acids (formate, acetate and oxalate) disappeared, indicating the mineralization of AB into CO_2.

Also, the photocatalytic mineralization of AB implies the appearance of inorganic products, mainly anions, since hetero-atoms are generally converted into anions in which they are at their highest oxidation degree. The removal of TOC (total organic carbon) is commonly employed to indicate the mineralization of organic pollutants. To quantitatively characterize the mineralization of AB and SF in the solution, the removal TOC ratio was used in this study. The TOC removal ratio is about 95 % after 240 min of irradiation. The overall stoichiometry for mineralization of AB and SF can be written as

(AB)

$$C_{20}H_{26}N_4O_6S_2 + 63H_2O_2 \rightarrow 20CO_2 + 4NO_3^- + 2SO_4^{2-} + 72H_2O + 8H^+ \quad (3)$$

(SF)

$$C_{28}H_{18}N_4O_6S_4Na_2 + 82H_2O_2 \rightarrow 28CO_2 + 4NO_3^- + 4SO_4^{2-} + 86H_2O + 10H^+ + 2Na^+ \quad (4)$$

Mineralization of AB and SF is reported for an irradiation period of 240 min. The formation of SO_4^{2-} and NO_3^- from AB and SF mineralization was shown in Figs. 3a and 3b, respectively. It can be seen from Figs. 3a and 3b that the amount of SO_4^{2-} and NO_3^- anions increased and gradually reached to a maximum as the irradiation time increasing, indicating that the selected dyes were mineralized. However, the quantity of sulfate ions released (0.18 and 0.26 mM for AB and SF, respectively) is lower than that expected from stoichiometry (0.22 and 0.29 mM for AB and SF, respectively). This could be first explained by a loss of sulfur-containing volatile compounds such as H_2S and/or SO_2. However, this is not probable since both gases are very soluble in water and known as readily oxidizable into sulfate by photocatalysis. The more probable explanation for the quantity of SO_4^{2-} obtained smaller than that expected from stoichiometry is given by the partially irreversible adsorption of some SO_4^{2-} ions at the surface of titania as already observed. However, this partial adsorption of SO_4^{2-} ions does not inhibit the photocatalytic degradation of pollutants [39]. Also, the quan-

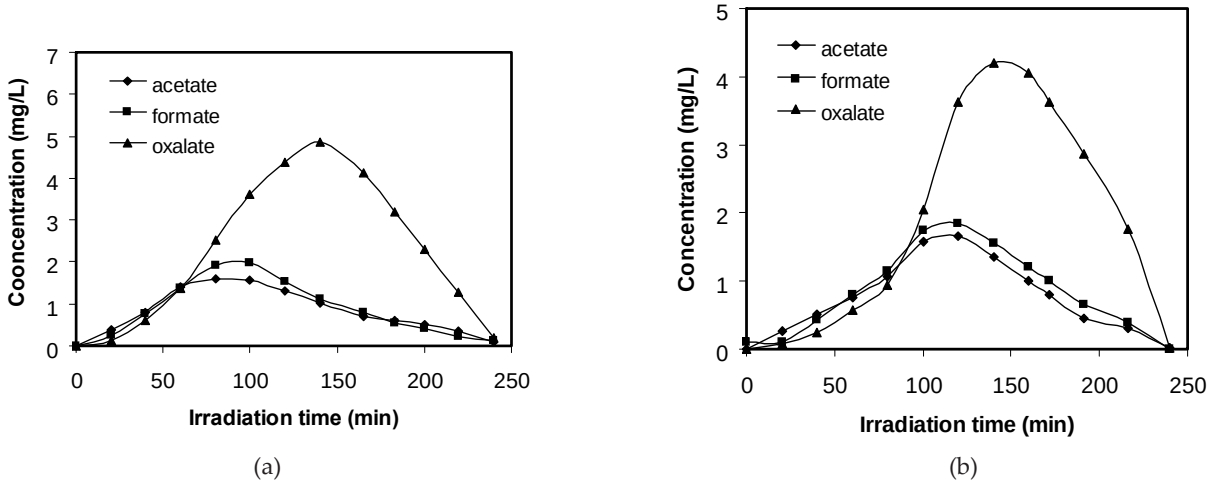

Fig. 2. Formation and disappearance of aliphatic carboxylic acids in the solution during the photocatalytic degradation of (a) AB (Dye: 0.11 mM, H_2O_2: 7.3 mM) and (b) SF (Dye: 0.073 mM, H_2O_2: 5.0 mM).

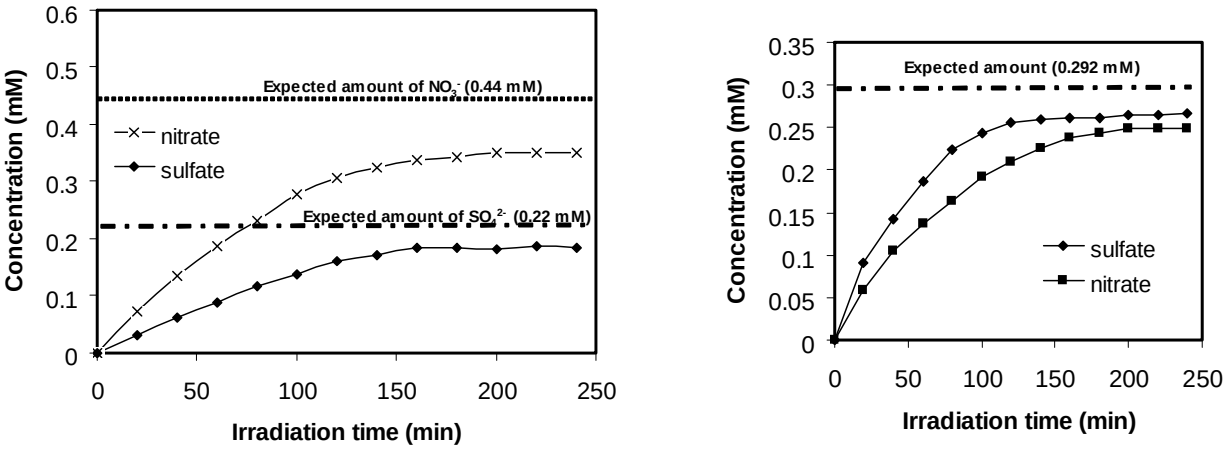

Fig. 3. Evolution of sulfate and nitrate anions during the photocatalytic mineralization of (a) AB (Dye: 0.11 mM, H_2O_2: 7.3 mM) and (b) SF (Dye: 0.073 mM, H_2O_2: 5.0 mM).

tity of nitrate ions released (0.35 and 0.25 mM for AB and SF, respectively) is lower than that expected from stoichiometry (0.44 and 0.29 mM for AB and SF, respectively) indicating that N-containing species remain adsorbed in the photocatalyst surface or most probably, that significant quantities of N_2 and/or NH_3 have been produced and transferred to the gas-phase. In azo bond each nitrogen atom is in its +1 oxidation degree. This oxidation degree favors the evolution of gaseous dinitrogen by the two step reduction process expressed previously. N_2 evolution constitutes the ideal case for a decontamination reaction involving totally innocuous nitrogen-containing final product [12].

4. Conclusions

The AB and SF dyes could be successfully decolorized and mineralized by photocatalysis in an immobilized TiO_2 particle photocatalytic reactor. Also, this paper presents a computational fluid dynamics model to simulate photocatalytic decolorization of AB and SF dyes from aqueous solution. The agreement between the predicted results and measured data are close. The photocatalytic decolorization kinetics follows a first-order model for both dyes. This technique may be a viable one for treatment of large volume of aqueous colored dye solutions.

References

[1] A. Aleboyeh, Y. Moussa and H. Aleboyeh, The effect of operational parameters on UV/H_2O_2 decolourisation of Acid Blue 74. Dyes Pigments, 66 (2005) 129–134.
[2] M. Arami, N.Y. Limaee and N.M. Mahmoodi, Investigation on the adsorption capability of egg shell membrane towards model textile dyes. Chemosphere, 65 (2006) 1999–2008.
[3] M. Arami, N.Y. Limaee, N.M. Mahmoodi and N.S. Tabrizi, Removal of dyes from colored textile wastewater by orange peel adsorbent: equilibrium and kinetics studies, J. Colloid Interface Sci., 288 (2005) 371–376.
[4] M. Arami, N.Y. Limaee, N.M. Mahmoodi and N.S. Tabrizi, Equilibrium and kinetics studies for the adsorption of direct and acid dyes from aqueous solution by soy meal hull, J. Hazard. Mater., 135 (2006) 171–179.
[5] C.H. Wu, Effects of operational parameters on the decolorization of C.I. Reactive Red 198 in UV/TiO_2-based systems. Dyes Pigments, 77 (2008) 31–38.
[6] M.A. Behnajady, N. Modirshahla, N. and M. Rabbani, Photocatalytic degradation of an azo dye in a tubular continuous-flow photoreactor with immobilized TiO_2 on glass plates. Chem. Eng. J., 127 (2007) 167–176.
[7] N.M. Mahmoodi, M. Arami, N.Y. Limaee and N.S. Tabrizi, Decolorization and aromatic ring degradation kinetics of Direct Red 80 by UV oxidation in the presence of hydrogen peroxide utilizing TiO_2 as a photocatalyst. Chem. Eng. J., 112 (2005) 191–196.
[8] N.M. Mahmoodi, M. Arami, N.Y. Limaee and N.S. Tabrizi, Kinetics of heterogeneous photocatalytic degradation of reactive dyes in an immobilized TiO_2 photocatalytic reactor. J. Colloid Interf. Sci., 295 (2006) 159–164.
[9] N.M. Mahmoodi and M. Arami, Modeling and sensitivity analysis of dyes adsorption onto natural adsorbent from colored textile wastewater. J. Appl. Polym. Sci., 109 (2008) 4043–4048.
[10] V. Luca, M. Osborne, D. Sizgek, C. Griffith and P.Z. Araujo, Photodegradation of methylene blue using crystalline titanosilicate quantum-confined semiconductor. Chem. Mater., 18 (2006) 6132–6138.
[11] M.R. Hoffmann, S.T. Martin, W. Choi and D.W. Bahneman, Environmental applications of semiconductor photocatalysis, Chem. Rev., 95 (1995) 69–96.
[12] I.K. Konstantinou and T.A. Albanis, TiO_2-assisted photocatalytic degradation of azo dyes in aqueous solution: kinetic and mechanistic investigations — a review, Appl. Catal. B: Environ., 49 (2004) 1–14.
[13] N.M. Mahmoodi, M. Arami, N.Y. Limaee and K. Gharanjig, Photocatalytic degradation of agricultural N-heterocyclic organic pollutants using immobilized nanoparticles of titania. J. Hazard. Mater., 145 (2007) 65–71.
[14] N.M. Mahmoodi, M. Arami, N.Y. Limaee, K. Gharanjig and F.D.

Ardejani, Decolorization and mineralization of textile dyes at solution bulk by heterogeneous nanophotocatalysis using immobilized nanoparticles of titanium dioxide. Colloids Surface A: Physicochem. Eng. Aspects, 290 (2006) 125–131.
[15] N.M. Mahmoodi and M. Arami, Bulk phase degradation of Acid Red 14 by nanophotocatalysis using immobilized titanium (IV) oxide nanoparticles. J. Photochem. Photobiol. A: Chem., 182 (2006) 60–66.
[16] M.Y. Ghaly, J.Y. Farah and A.M. Fathy, Enhancement of decolorization rate and COD removal from dyes containing wastewater by the addition of hydrogen peroxide under solar photocatalytic oxidation. Desalination, 217 (2007) 74–84.
[17] N. Kuburovic, M. Todorovic, V. Raicevic, A. Orlovic, L. Jovanovic, J. Nikolic, V. Kuburovic, S. Drmanic and T. Solevic, Removal of methyl tertiary butyl ether from wastewaters using photolytic, photocatalytic and microbiological degradation processes. Desalination, 213 (2007) 123–128.
[18] L. Rizzo, J. Koch, V. Belgiorno and M.A. Anderson, Removal of methylene blue in a photocatalytic reactor using polymethylmethacrylate supported TiO_2 nanofilm. Desalination, 211 (2007) 1–9.
[19] C.S. Uyguner, S.A. Suphandag, A. Kerc and M. Bekbolet, Evaluation of adsorption and coagulation characteristics of humic acids preceded by alternative advanced oxidation techniques. Desalination, 210 (2007) 183–193.
[20] F.H. Hussein and A.N. Alkhateeb, Photo-oxidation of benzyl alcohol under natural weathering conditions. Desalination, 209 (2007) 350–355.
[21] J.Q. Chen, D. Wang, M.X. Zhu and C.J. Gao, Photocatalytic degradation of dimethoate using nanosized TiO_2 powder. Desalination, 207 (2007) 87–94.
[22] C. Sahoo, A.K. Gupta and A. Pal, Photocatalytic degradation of Methyl Red dye in aqueous solutions under UV irradiation using Ag^+ doped TiO_2. Desalination, 181 (2005) 91–100.
[23] N.H. Salah, M. Bouhelassaa, S. Bekkouche and A. Boultii, Study of photocatalytic degradation of phenol. Desalination, 166 (2004) 347–354.
[24] M. Toyoda, Y. Nanbu, T. Kito, M. Hiranob anf M. Inagaki, Preparation and performance of anatase-loaded porous carbons for water purification. Desalination, 159 (2003) 273–282.
[25] K.M. Reddy, S.V. Manorama and A.R. Reddy, Bandgap studies on anatase titanium dioxide nanoparticles. Mater. Chem. Physics, 78 (2002) 239–245.
[26] X. Chen and S.S. Mao, Titanium dioxide nanomaterials: Synthesis, properties, modifications and applications. Chem. Rev., 107 (2007) 2891–2959.
[27] X. Chen and S.S. Mao, Synthesis of titanium dioxide (TiO_2) nanomaterials. J. Nanosci. Nanotechnol., 6 (2006) 906–925.
[28] A.K. Ray and A.A.C.M. Beenackers, Novel photocatalytic reactor for water treatment. AIChE J., 44 (1998) 477–483.
[29] N.M. Mahmoodi, M. Arami, K. Gharanjig, F. Nourmohammadian and A.Y. Bidokhti, Purification of water containing agricultural organophosphorus pollutant using titania nanophotocatalysis: Laboratory studies and numerical modeling. Desalination, 230 (2008) 183–192.
[30] J. Mackerle, Finite element modeling and simulations in cardiovascular mechanics and cardiology: a bibliography 1993-2004. Comput. Methods Biomech. Biomed. Eng., 8 (2005) 59–81.
[31] J. Mackerle, Finite element modeling and simulations in dentistry: a bibliography 1990–2003. Comput. Methods Biomech. Biomed. Eng., 7 (2004) 277–303.
[32] J.S. Raul, D. Baumgartner, R. Willinger and B. Ludes, Finite element modelling of human head injuries caused by a fall. Int. J. Legal Med., 120 (2006) 212–218.
[33] N.M. Mahmoodi, M. Arami, N.Y. Limaee, K. Gharanjig and F. Nourmohammadian, Nanophotocatalysis using immobilized titanium dioxide nanoparticle. Degradation and mineralization of water containing organic pollutant: case study of Butachlor. Mater. Res. Bull., 42 (2007) 797–806.
[34] N.M. Mahmoodi, N.Y. Limaee, M. Arami, S. Borhany and M. Mohammad-Taheri, Nanophotocatalysis using nanoparticles of titania. Mineralization and finite element modelling of Solophenyl dye decolorization. J. Photochem. Photobiol. A: Chem., 189 (2007) 1–6.
[35] N.M. Mahmoodi, M. Arami and N.Y. Limaee, Photocatalytic degradation of triazinic ring-containing azo dye (Reactive Red 198) by using immobilized TiO_2 photoreactor: Bench scale study. J. Hazard. Mater., 133 (2006) 113–118.
[36] C.M. So, M.Y. Cheng, J.C. Yu and P.K. Wong, Degradation of azo dye Procion Red MX-5B by photocatalytic oxidation, Chemosphere, 46 (2002) 905–912.
[37] CHAM (2000), The PHOENICS On-Line Information System, http://www.cham.co.uk/ phoenics /d_polis/polis.htm.
[38] A. Houas, H. Lachheb, M. Ksibi, E. Elaloui, C. Guillard and J.M. Hermann, Photocatalytic degradation pathway of Methylene Blue in Water. Appl. Catal. B: Environ., 31 (2001) 145–157.
[39] K. Tanaka, S.M. Robledo, T. Hisanaga, R. Ali, Z. Ramli and W.A. Bakar, Photocatalytic degradation of 3,4-xylyl N-methylcarbamate (MPMC) and other carbamate pesticides in aqueous TiO_2 suspensions. J. Mol. Catal. A: Chem., 144 (1999) 425–430.